Journal of the Optical Society of Korea
Vol. 19, No. 5, October 2015, pp. 449-455

ISSN: 1226-4776(Print) / ISSN: 2093-6885(Online)
DOI: http://dx.doi.org/10.3807/JOSK.2015.19.5.449

Hybrid Square-Lattice Photonic Crystal Fiber with Broadband Single-Mode Operation, High Birefringence, and Normal Dispersion

Soeun Kim[1†], Yong Soo Lee[1], Chung Ghiu Lee[2], Yongmin Jung[3], and Kyunghwan Oh[4*]

[1]*Integrated Optics Laboratory, Advanced Photonics Research Institute, GIST, Gwangju 500-712, Korea*
[2]*Department of Electronic Engineering, Chosun University, Gwangju 501-759, Korea*
[3]*Optoelectronics Research Centre, University of Southampton, Highfield, Southampton, SO17 1BJ, UK*
[4]*Departmemt of Physics, Yonsei University, Seoul 120-749, Korea*

(Received July 3, 2015 : revised August 19, 2015 : accepted September 8, 2015)

In this study we propose a new photonic crystal fiber (PCF) design that simultaneously offers broadband single-mode operation, high birefringence, and large normal dispersion in the optical-communication wavelength regime. The waveguide is based on a hybrid square-lattice PCF (HS-PCF) that has circular air holes of two different diameters alternating in the cladding, plus a pure silica defect at the center. The optical properties of the guided modes are analyzed numerically by the finite-element method (FEM) with a perfectly matched layer as the boundary condition. The optimized HS-PCF has a dispersion coefficient of -601.67 ps nm^{-1} km^{-1} and a high birefringence of 1.025×10^{-2} at 1.55 μm. In addition, over the S+C+L+U wavelength bands the proposed HS-PCF with ultraflat birefringence with a slope on the order of 10^{-5}.

Keywords : Photonic crystal fiber, High birefringence, Normal dispersion
OCIS codes : (060.2270) Fiber characterization; (060.2280) Fiber design and fabrication; (060.5295) Photonic crystal fibers

I. INTRODUCTION

Simultaneous achievement of high birefringence, broadband normal dispersion, and endlessly single-mode operation for an optical fiber would provide a new platform for optical communications and optical-fiber sensing systems. By controlling polarization cross-talk, high birefringence in fiber optics has found various applications in fiber-optic sensors, gyroscopes, interferometers, fiber lasers, and coherent optical communications [1, 2]. Broadband normal dispersion in an optical fiber is needed to compensate for chromatic dispersion in a conventional single-mode fiber (SMF) over a wide range of wavelengths in wavelength-division multiplexed communication systems [3]. In addition, stable single-mode operation in photonic waveguides is a fundamental requirement in many areas of modern photonics and optical communications systems, and broadband operation with single-mode guidance is very important for improving overall system performance. Several types of optical fibers with a conventional step-index design have been proposed to address these issues individually, but there has been no integrated solution that addresses all of these issues simultaneously. An integrated solution to combining various optical functions (*i.e.* multipurpose optical waveguide) not only could enhance system performance, but also could initiate a new class of optical components. However, simultaneous control of light polarization, dispersion, and single-mode operation is not easy, because there is a tradeoff between these three properties in conventional step-index optical fibers. In recent years photonic crystal fibers (PCFs) have been widely investigated due to their unique optical properties such as high birefringence, anomalous dispersion, and single-mode operation [4-8], which cannot be achieved in conventional optical fibers. Due to their greatly enhanced index contrast, PCFs can easily achieve very high birefringence (HB), and various HB-PCF designs have been reported with asymmetric defect structures such as dissimilar air holes along the two orthogonal axes [6, 9], asymmetric defect cores [10-11], elliptical-hole PCFs (EPCFs) [12], and squeezed-lattice PCFs [13-14]. The birefringence of these HB-PCFs ranges from 10^{-3} to 10^{-2}, one

*Corresponding authors: koh@yonsei.ac.kr, †sekim@gist.ac.kr
Color versions of one or more of the figures in this paper are available online.

to two orders of magnitude higher than in conventional HB fibers [15]. Due to the difficulty of fabricating noncircular air holes, most HB-PCFs have been extensively designed with only circular air holes by breaking the cylindrical symmetry of the fiber [6, 9-11]. In previous HB-PCFs, high birefringence could be achieved easily due to the greatly enhanced refractive-index contrast. In general, higher refractive-index contrast helps to increase the birefringence of the fiber, but it results in excessive chromatic dispersion and higher-order mode guidance (*i.e.* becoming a multimode waveguide). For example, hexagonal air-silica PCFs with circular air holes have exhibited endlessly single-mode operation for a certain conditions of hole diameter d and pitch Λ: $d/\Lambda < 0.45$ [5]. However, higher birefringence in a PCF requires a larger d/Λ (> 0.45), and it is very difficult to obtain high birefringence and broadband, large normal dispersion while preserving single-mode operation. Therefore, previous HB-PCFs could not provide high birefringence, large normal dispersion, and single-mode operation at the same time. Recently, special PCF designs have been proposed to control several optical properties simultaneously [17, 18], but require very sophisticated manufacturing to realize a complex fiber cross section with various sizes of air holes and a spiral lattice structure.

In this study we propose a hybridsquare-lattice PCF based on the conventional square lattice and just two different-size air holes to control various optical properties simultaneously such as high birefringence, large normal dispersion, and single-mode operation. The proposed PCF has circular air holes of two different diameters alternating in the cladding, plus a silica defect at the center. Preliminary results for the proposed design have been published in conference proceedings [19-21]. However, in this paper, we show progress in control of multiple optical properties such as high birefringence, large normal dispersion, and single-mode operation at the same time. The optical properties of the guided modes are analyzed numerically by the finite-element method with a perfectly matched layer as the boundary condition. The proposed fiber structure is based on the conventional square-lattice cladding, which can be readily fabricated by the stack-and-draw method using fused-silica glass capillaries of two different wall thicknesses [4].

II. DESIGN METHODOLOGY

The new PCF design in this study is based on a hybrid-square-lattice cladding structure. The core of the HS-PCF is based on that of a conventional HB-PCF. To illustrate the design algorithm for a proposed fiber, the cross sections of a proposed HS-PCF and a conventional HB-PCF are shown in Figs. 1(a) and (b) respectively. Both PCFs have a central silica defect and smaller air holes on both sides, which introduce asymmetry in the core. The lattice of the cladding region is defined by the distance between consecutive holes Λ, the larger hole diameter d_1, and the smaller hole diameter

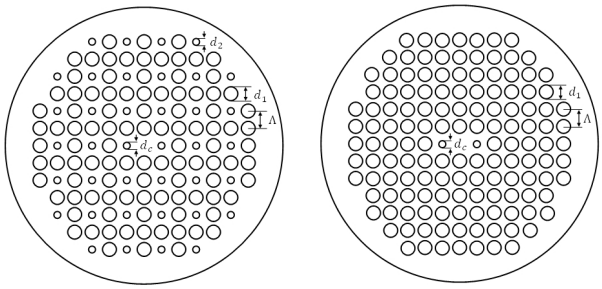

FIG. 1. Transverse cross section of (a) the proposed HS-PCF and (b) a conventional HB-PCF. Both PCFs have the same structural parameters Λ, d_1, d_c, and d_2.

d_2. The defected core is defined by the central air-hole diameter d_c. Both PCFs start from two common structural facts: First, the lattice structure of the cladding is set to be a conventional square lattice with a small Λ of about 1 μm, to obtain normal dispersion. The small Λ based on the square lattice was chosen according to the report of Bouk *et al*. [22], which demonstrated that a square-lattice PCF with a small Λ of about 1 μm exhibited normal dispersion at a wavelength of 1.55 μm. Second, the central silica defect and smaller air holes on both sides are introduced to both PCFs to provide the asymmetry needed to achieve high birefringence. An asymmetric core is generally used for an HB-PCF. The only difference in fiber design between a conventional HB-PCF and the proposed HS-PCF is the presence of smaller air holes in the cladding of the HS-PCF, to optimize the refractive-index contrast between core and cladding for single-mode operation. The cladding structure is varied to control optical properties because the cladding structure does not have a decisive effect on the high birefringence value, if the asymmetry of the core is maintained.

III. COMPARATIVE STUDY OF A CONVENTIONAL HB-PCF AND THE PROPOSED HS-PCF

To demonstrate the effect of smaller air holes in the cladding of the proposed HS-PCF on its modal properties, we compared the modal properties of a conventional HB-PCF and a proposed HS-PCF using the finite-element method (FEM) with the circular perfectly matched layer (PML) boundary condition. An efficient boundary condition must be used to simulate the leakage. PMLs are the most efficient absorption boundary conditions, producing no reflection at the boundary [23].

In an optical fiber with mode guiding by total internal reflection (TIR), single-mode operation is cut off when the effective refractive index of the guided mode becomes equal to the effective index of the fundamental space-filling mode of the cladding [5]. Using FEM, the effective indices of

guided modes and the cladding mode can be swept as a function of the wavelength. We found the crossing point as a cutoff wavelength by plotting the effective index of each mode obtained by FEM. Figure 2 shows the modal dispersion curves for the guided modes and cladding modes for the proposed HS-PCF (Fig. 2(a)) and the conventional HB-PCF (Fig. 2(b)) with $\Lambda = 1$ μm, $d_1/\Lambda = 0.8$, and $d_c/\Lambda = d_2/\Lambda = 0.4$. To increase field confinement, here d_1/Λ is chosen to be a large value of 0.8. In this case the cutoff wavelength for single-mode operation in the proposed HS-PCF is 1.332 μm. Therefore, over S+C+L wavelength bands the HS-PCF is a true single-mode fiber, supporting only the LP_{01} mode. However, a conventional HB-PCF supports both the fundamental mode and the second-order hybrid modes LP_{01} and LP_{11} over the wavelength range for optical communication. To compare the dispersion relations of the two fibers in detail, we overlaid the two plots. Figure 2(c) shows that the black solid and dashed lines of *x*- and *y*-polarized modes for both PCFs overlap completely. Guided higher modes also overlap. This means that the guiding modes for both PCFs show the same behavior, because they have almost the same core design, while the effective index of the fundamental cladding mode of the proposed HS-PCF (red solid line) is larger than that of the conventional HB-PCF (red dashed line), the small air holes introduced into the cladding resulting in single-mode operation.

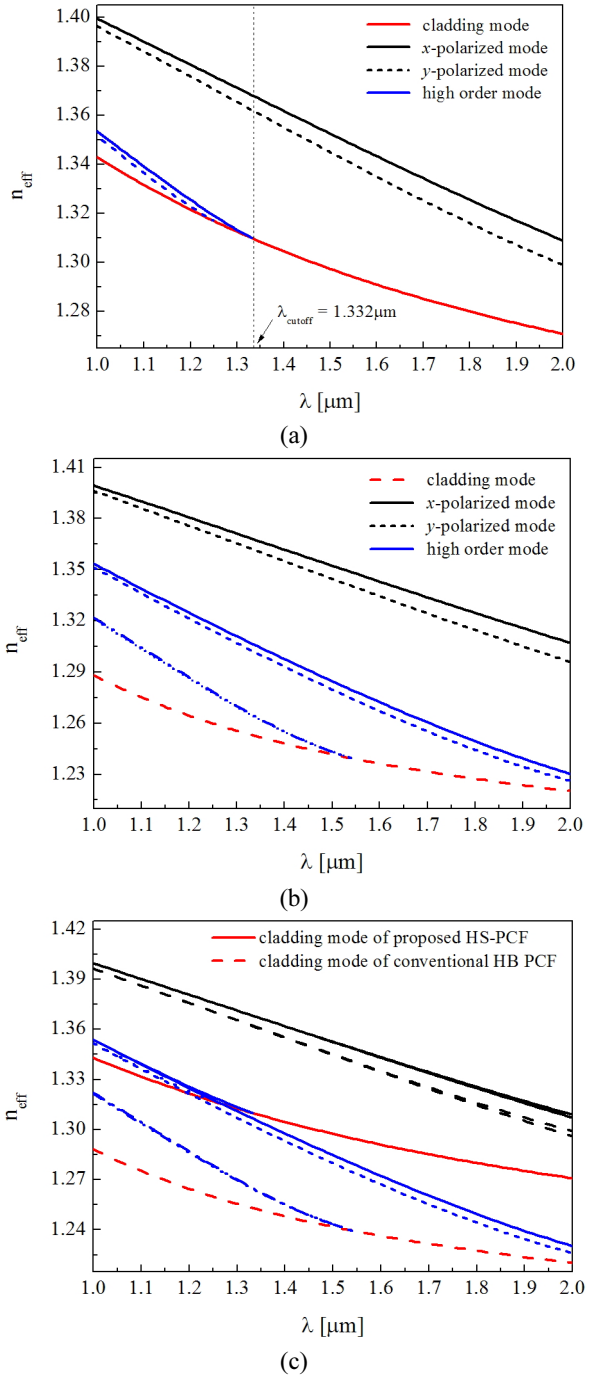

FIG. 2. Modal dispersion curves as a function of wavelength for (a) the proposed HS-PCF and (b) a conventional HB-PCF, where $\Lambda = 1$ μm, $d_1/\Lambda = 0.8$, and $d_c/\Lambda = d_2/\Lambda = 0.4$. (c) = (a) + (b).

Reducing the index contrast between core and cladding by adding small air holes in the cladding is a simple design strategy for a HS-PCF to yield a single-mode fiber while maintaining high birefringence. This is a key result, and the reason to introduce small air holes into the cladding for a proposed HS-PCF.

Next, to study the effect of small air holes in the cladding of the HS-PCF on its optical properties, the guided-mode shape, modal birefringence, chromatic dispersion, and confinement loss of the fundamental modes for both HB-PCFs are numerically analyzed. Once the modal complex effective index n_{eff} and electric fields are obtained by FEM, the birefringence, chromatic dispersion, and confinement loss can be calculated using the following relations:

$$D = -\frac{\lambda}{c}\frac{d^2 Re[n_{eff}]}{d\lambda^2} \tag{1}$$

$$B = \left| n_{eff_x} - n_{eff_y} \right| \tag{2}$$

where $Re[n_{eff}]$ is the real part of the effective refractive index n_{eff}, λ is the wavelength of light, and c is the velocity of light in vacuum. $Im[k_0\, n_{eff}]$ is the imaginary part of $k_0\, n_{eff}$, with $k_0 = 2\pi/\lambda$ being the free-space wave number. The material dispersion given by the Sellmeier formula is directly included in the calculation; therefore, D in (1) corresponds to the total dispersion of the PCF.

Figure 3 shows the *x*- and *y*-polarized fundamental modes of both HB-PCFs at 1.55 μm, where $\Lambda = 1$ μm, $d_1/\Lambda = 0.8$, and $d_c/\Lambda = d_2/\Lambda = 0.4$. The numerical results show that the *x*- and *y*-polarized fundamental modes for the conventional HB-PCF (Figs. 3(a) and (b)) and the proposed HS-PCF (Figs. 3(c) and (d)) are strongly bounded in the core region, with $B = 7.97\times10^{-3}$ and 8.02×10^{-3} respectively. The remarkable point from these results is that the mode distributions for both HB-PCFs are almost unaffected by their different

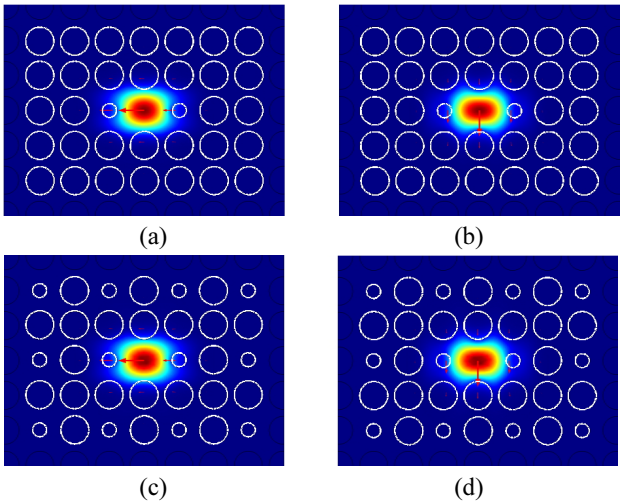

FIG. 3. Mode field distributions of (a), (c) *x*- and (b), (d) *y*-polarized modes for (a), (b) the proposed HS-PCF and (c), (d) a conventional HB-PCF.

cladding structures.

To compare other optical properties of both PCFs, the modal birefringence and chromatic dispersion of the *x*-polarized mode as a function of wavelength, defined by equations (1) and (2), for both HB-PCFs are shown in Fig. 4. Here the red and black lines are the results for the proposed HS-PCF and conventional HB-PCF respectively, with solid lines showing the *x*-polarized fundamental mode and dashed lines the *y*-polarized fundamental mode in Fig. 4(b). The birefringence of the HS-PCF becomes slightly lower than that of the conventional HB-PCF as the wavelength increases. However, the difference in birefringence between both PCFs is extremely small, about 10^{-5}, which is negligible. This predictable result is due to the lower index contrast between core and cladding, obtained by introducing smaller air holes in the cladding for the proposed HS-PCF. On the other hand, the normal dispersion of the proposed HS-PCF is enhanced in comparison to the conventional HB-PCF. Due to the smaller air holes in the cladding, the proposed HS-PCF has lower effective index contrast between core and cladding [24], and the fiber can provide larger normal dispersion than a conventional HB-PCF. The values of dispersion for the *y*-polarized mode of the conventional HB-PCF and the proposed HS-PCF are -82.06 and -136.2 ps nm^{-1} km^{-1} at 1.55 μm, respectively.

Now we discuss the confinement losses of the two PCFs. As expected, the confinement loss for the HS-PCF becomes slightly greater than that for the conventional HB-PCF, because of the lower index contrast between core and cladding. However, the confinement loss is still quite small (< 0.205 dB/km) and comparable to that of a conventional SMF. From the simulation results, the proposed HS-PCF shows slightly lower birefringence and higher confinement loss than the conventional HB-PCF. However, there is a key advantage in the proposed HS-PCF beyond the conventional HB-PCF: The HS-PCF can support true single-mode operation over

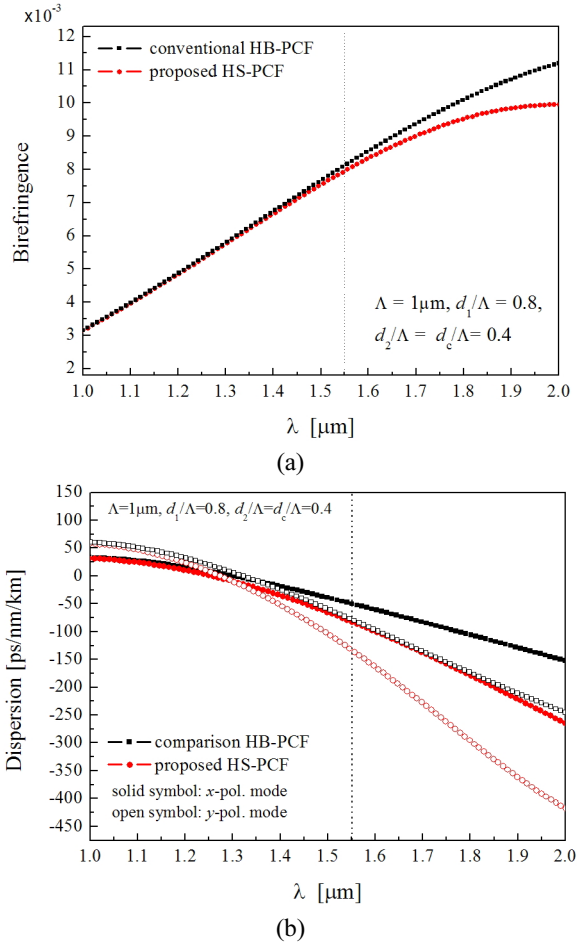

FIG. 4. Comparison of (a) birefringence and (b) dispersion of *x*- and *y*-polarized modes as a function of wavelength for the proposed HS-PCF and a conventional HB-PCF, with Λ = 1 μm, $d_1/\Lambda = 0.8$, and $d_2/\Lambda = d_c/\Lambda = 0.4$.

the entire communication band, with high birefringence and normal dispersion at the same time.

IV. OPTIMIZATION OF THE PROPOSED HS-PCF

To apply the proposed HS-PCF to an optical communication system, the optical properties of the proposed fiber should be optimized over the S, C, and L communication bands. Figs. 5(a) and (b) show the effects of the structural parameters Λ and d_2/Λ, respectively, on the birefringence and chromatic dispersion of *x*-and *y*-polarized modes at λ = 1.55 μm. Fig. 5(c) shows the cutoff conditions for single-mode operation for various values of d_2/Λ, where the fixed parameters are d_c/Λ = 0.4, d_1/Λ =0.8, and Λ = 0.752 μm. In Fig. 5(a), polarization maintenance and dispersion compensation are improved by decreasing Λ. Remarkably, the birefringence is highest and becomes flattened for 0.752 μm < Λ < 0.772 μm. When Λ = 0.752 μm, the birefringence

and dispersion for the HS-PCF are optimized as 1.02×10^{-2} and -586.80 ps nm^{-1} km^{-1}, respectively. Next, we changed d_2/Λ in the cladding; the results are shown in Fig. 5(b) for $\Lambda = 0.752$ μm, $d_c/\Lambda = 0.4$, and $d_1/\Lambda = 0.8$. With increasing d_2/Λ, the birefringence becomes higher and the normal dispersion lower. When d_2/Λ becomes 0.8, the proposed HS-PCF is the same as the conventional HB-PCF. Therefore, a study of the cutoff condition for d_2/Λ is required to find an optimized single-mode PCF maintaining high birefringence and normal dispersion simultaneously. The cutoff wavelength for single-mode operation is simulated by varying d_2/Λ, and plotted in Fig. 5(c). Other parameters are fixed: $\Lambda = 0.752$ μm, $d_1/\Lambda = 0.8$, and $d_c/\Lambda = 0.4$. The blue dashed line indicates $\lambda_{cutoff} = 1.55$ μm. As shown in Fig. 5(c), when $d_2/\Lambda < 0.7$ the proposed HS-PCF guides only the fundamental mode. From the above results, it is very worthwhile to find the optimized parameters for simultaneous true single-mode operation, high birefringence, and normal dispersion. The optimized Λ for highest birefringence in Fig. 5(a) is 0.752 μm, where $d_1/\Lambda = 0.8$ and $d_2/\Lambda = d_c/\Lambda = 0.4$.

The optimized d_2/Λ is set to be 0.4 for high normal dispersion and wide-band single-mode operation above a wavelength of 1.0 μm. The result is shown in Fig. 6. It can be seen that the optimized HS-PCF has a normal dispersion

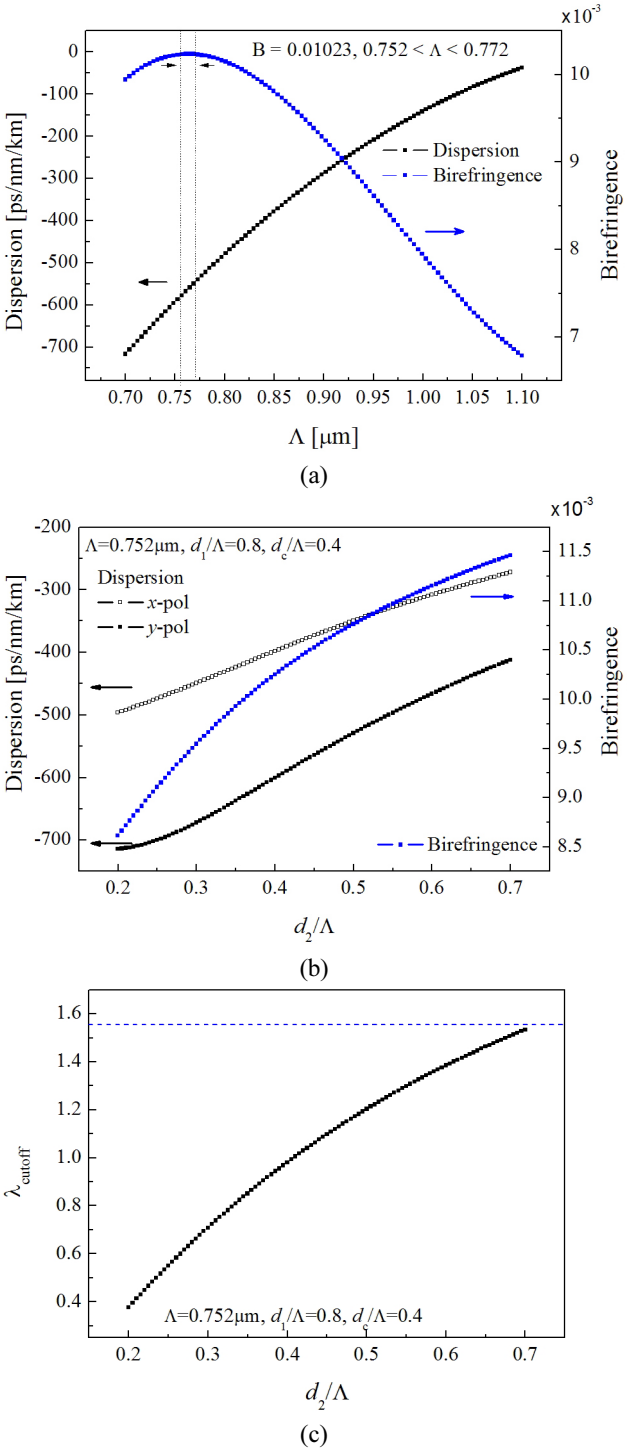

FIG. 5. Effect of (a) Λ and (b) d_2/Λ on birefringence and dispersion of the proposed HS-PCF. (c) Cutoff condition for single-mode operation for the proposed HS-PCF for various values of d_2/Λ.

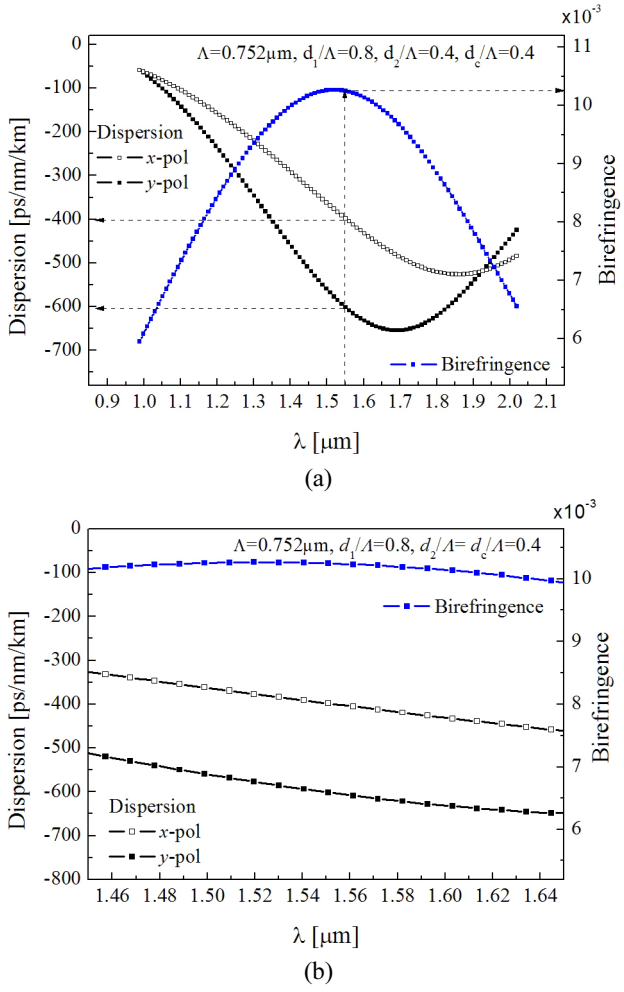

FIG. 6. (a) Birefringence and dispersion as a function of wavelength for the optimized HS-PCF with $\Lambda = 0.752$ μm, $d_1/\Lambda = 0.8$, and $d_2/\Lambda = d_c/\Lambda = 0.4$. (b) Ultraflat high birefringence over S+C+L+U wavelength bands.

coefficient of -601.67 ps nm^{-1} km^{-1} for the *y*-polarized mode and maximum birefringence of 1.025×10^{-2} at 1.55 μm. Fig. 6(b), an expanded plot of Fig. 6(a), shows that the value of birefringence with optimized parameters is ultraflat over the wavelength range 1.45-1.65 μm, with slope of the order of 10^{-5}.

According to the above results, the proposed HS-PCF can act as a DCF to compensate for the accumulated dispersion of an SMF, and can be used to eliminate the effect of PMD in optical communication systems, and in many other areas where polarization-maintaining properties are required, such as sensing applications [25]. Fibers with highly flat birefringence and dispersion compensation are extensively used in fiber-loop mirrors, as a major component for optical-fiber sensing applications, with better performance for fiber-sensor design. In addition, true single-mode operation is also required for a long-distance data transmission system.

A simple fabrication process is a key advantage for a PCF. Other HB-PCFs, dispersion-compensating PCFs, or PCFs with both properties, have very complicated structures to enhance performance, such as elliptical air holes [12], five types of different air holes, and unconventional cladding structure [13-14, 25], which are difficult to fabricate using the stack-and-draw method. Another strong point of the proposed HS-PCF design is its easy fabrication process. All the air holes of the HS-PCF are circular, and the structure of the cladding is a conventional square lattice. Therefore, using the conventional stack-and-draw method, the proposed HS-PCF can be easily fabricated [26-29]. The most important issue in the optical-communication industry lately has been the reduction of price in the development of optical devices. To accoplish this, the functions of various optical components should be combined in a single device, to minimize the system. The proposed HS-PCF is a good example of a combined integrated waveguide with the multiple functions of polarization maintenance, broadband dispersion compensation, low loss, and true single-mode operation for optical-communication and smart-sensing applications.

V. CONCLUSIONS

In this paper we have proposed a true single-mode, highly birefringent, and broadband dispersion-compensating HS-PCF over a wideband optical-communication region. By the simple design strategy of introducing small air holes into the cladding of a conventional HB-PCF, broadband single-mode operation, high birefringence, and large normal dispersion can be achieved simultaneously in the proposed HS-PCF. The optimized HS-PCF has a normal dispersion coefficient of -601.67 ps nm^{-1} km^{-1} and birefringence of 1.025×10^{-2} at 1.55 μm. In addition, in the S+C+L+U wavelength bands the proposed HS-PCF has ultraflat birefringence with a slope of the order of 10^{-5}. The confinement loss of this HS-PCF is comparable to that of a conventional SMF, according to numerical results using an imaginary effective index. The proposed HS-PCF can be used as a multifunction waveguide in optical-communication and smart-optical-sensor applications.

ACKNOWLEDGMENT

This work was supported by The Asian Laser Center Program of Gwangju Institute of Science and Technology.

REFERENCES

1. R. A. Bergh, H. C. Lefevre, and H. J. Shaw, "An overview of fiber-optic gyroscopes," IEEE J. Lightwave Technol. **2**, 91-107 (1984).
2. M. Nakazawa, "Highly efficient Raman amplification in a polarization-preserving optical fiber," Appl. Phys. Lett. **46**, 628-630 (1985).
3. K. Thyagarajan. R. K. Varshney, P. Palai, A. K. Ghatak, and I. C. Goyal, "A novel design of a dispersion compensating fiber," IEEE Photon. Technol. Lett. **8**, 1510-1512 (1996).
4. J. C. Knight, T. A. Birks, P. St. J. Russell, and D. M. Atkin, "All-silica single-mode optical with photonic crystal cladding," Opt. Lett. **21**, 1547-1549 (1996).
5. T. Birks, J. Knight, and P. Russell, "Endlessly single mode photonic crystal fiber," Opt. Lett. **22**, 961 (1997).
6. A. Ortigosa-Blanch, J. C. Knight, W. J. Wadsworth, J. Arriaga, B. J. Mangan, T. A. Birks, and P. St. J. Russell, "Highly birefringent photonic crystal fibers," Opt. Lett. **25**, 1325-1327 (2000).
7. A. Ferrando, E. Silvestre, J. J. Miret, and P. Andres, "Nearly zero ultraflattened dispersion in photonic crystal fiber," Opt. Lett. **25**, 790-792 (2000).
8. T. Matsui, K. Nakajima, and I. Sankawa, "Dispersion compensation over all the telecommunication bands with double-cladding photonic crystal fiber," IEEE J. Lightwave Technol. **25**, 757-762 (2007).
9. J. Ju, W. Jin, and M. S. Demokan, "Properties of a highly birefringent photonic crystal fiber," IEEE Photon. Technol. Lett. **15**, 1375-1377 (2003).
10. T. P. Hansen, J. Broeng, S. E. B. Libori, E. Knuders, A. Bjarklev, J. R. Jensen, and H. Simonsen, "Highly birefringent index-guiding photonic crystal fibers," IEEE Photon. Technol. Lett. **13**, 588-590 (2001).
11. S. Kim, C.-S. Kee, J. Lee, Y. Jung, H.-G. Choi, and K. Oh, "Ultrahigh birefringence of elliptic core fiber with irregular air holes," J. Appl. Phys. **101**, 016101 (2007).
12. M. J. Steel and P. M. Osgood Jr., "Elliptical-hole photonic crystal fibers," Opt. Lett. **26**, 229-231 (2001).
13. L. Zhang and C. Yang, "Photonic crystal fibers with squeezed hexagonal lattice," Opt. Express **12**, 2371-2376 (2004).
14. P. Song, L. Zhang, Z. Wang, Q. Hu, S. Zhao, S. Jiang, and S. Liu, "Birefringence characteristics of squeezed lattice photonic crystal fiber," IEEE J. Lightwave Technol. **25**, 1771-1776 (2007).
15. J. Noda, K. Okamoto, and Y, Sasaki, "Polarization maintaining fibers and their applications," IEEE J. Lightwave Technol. **4**, 1071-1089 (1986).

16. D. Chen, M.-L. V. Tse, and H. Y. Tam, "Super-lattice structure photonic crystal fiber," Prog. Electromagn. Res. M **11**, 53-64 (2010).
17. M. I. Hasan, M. Selim Habibb, M. Samiul Habibb, S. M. A. Razzakb, "Highly nonlinear and highly birefringent dispersion compensating photonic crystal fiber," Opt. Fiber Technol. **20**, 32-38 (2014).
18. M. A. Islam and M. S. Alam, "Design optimization of equiangular spiral photonic crystal fiber for large negative flat dispersion and high birefringence," IEEE J. Lightwave Technol. **30**, 3545-3551 (2012).
19. S. Kim, C. Kee, and C. G. Lee, "Hybrid square lattice photonic crystal fiber," in *Proc. Conference on Lasers and Electro-Optics/Pacific Rim* (Shanghai, China, 2009), TUP11_10.
20. S. Kim, C. G. Lee, I. Moon, and C.-S. Kee, "Hybrid square-lattice photonic crystal fiber with high birefringence and negative dispersion," Proc. SPIE **8421**, OFS 2012, 22nd International Conference on Optical Fiber Sensors, 842172 (2012).
21. S. Kim, Y. S. Lee, C.-S. Kee, and C. G. Lee, "Hybrid lattice photonic crystal fiber," in *Proc. 18th European Conference on Network and Optical Communications & 8th Conference on Optical Cabling and Infrastructure - NOC/OC&I 2013*, ISBN: 978-1-4673-5822-4 (Graz, Austria, 2013), pp. 1-4.
22. A. H. Bouk, A. Cucinotta, F. Poli, and S. Selleri, "Dispersion properties of square-lattice photonic crystal fibers," Opt. Express **12**, 941-946 (2001).
23. S. Guo, F. Wu, S. Albin, H. Tai, and R. S. Rogowski, "Loss and dispersion analysis of micro structured fibers by finite difference method," Opt. Express **12**, 3341-3352 (2004).
24. G. P. Agrawal, *Fiber-Optic Communication Systems* (Willey Inter-Science).
25. J. Park, S. Lee, S. Kim, and K. Oh, "Enhancement of chemical sensing capability in a photonic crystal fiber with a hollow high index ring defect at the center," Opt. Express **19**, 1921-1929 (2011).
26. R. Buczynski, "Photonic crystal fibers," Acta Physica Polonica A **106**, 141-167 (2004).
27. R. Buczynski, P. Szarniak, D. Pysz, I. Kujawa, R. Stepien, and T. Szoplik, "Double-core photonic crystal fiber with square lattice," Proc. SPIE **5450**, 223-230 (2004).
28. F. Couny, P. J. Roberts, T. A. Birks, and F. Benabid, "Square-lattice large-pitch hollow-core photonic crystal fiber," Opt. Express **16**, 20626-20636 (2008).
29. J. R. Hayes, J. C. Flanagan, T. M. Monro, D. J. Richardson, P. Grunewald, and R. Allott, "Square core jacketed air-clad fiber," Opt. Express **14**, 10345-10350 (2006).